Toward Closed-Loop Control of Pneumatic Grippers During Pack-and-Deploy Operations

Michelle Ching-Sum Yuen , Trevor R. Lear, Henry Tonoyan, Maria Telleria, and Rebecca Kramer-Bottiglio

Abstract—Soft robotic grippers can grasp objects of many different shapes while tolerating misalignments. However, many current soft systems lack proprioception and the ability to sense the position and orientation of the object to be grasped. Understanding the configuration of a gripper's fingers and the contact forces on a grasped object is crucial for manipulating an object and for interacting with the external environment. In this letter, we instrument a fabric-based pneumatic gripper with strain and pressure (force) sensors. Using sensors affixed to removable sleeves fit over each gripper finger, we identify the finger position and contact force on a grasped object. We show that we are able to completely deflate and pack the gripper, and then deploy the gripper and sensors to full operation. Finally, we demonstrate closed-loop control of the gripper configuration using the strain sensors to reconstruct pose.

Index Terms—Soft material robotics, grippers and other end-effectors, hydraulic/pneumatic actuators.
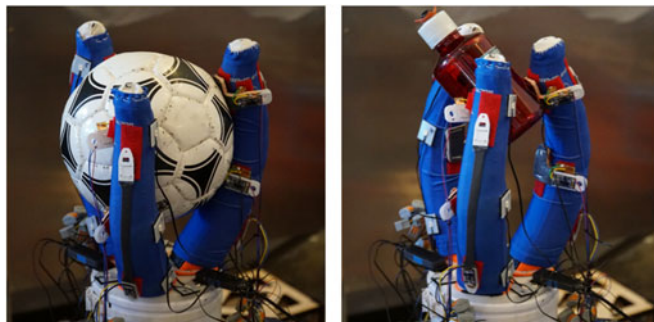

Fig. 1. The fabric-based pneumatic gripper conforming to grasp differently shaped objects. Strain sensors are attached along the outside of each finger. Two pressure sensors are affixed to the inside of each finger near the tip and in the middle.

I. INTRODUCTION

SOFT robotic grippers operate by deforming and conforming around objects to grasp them securely. This adaptability is made possible by using soft and flexible materials such as silicone elastomers [1]–[3], stretchable polymers [4], polymer-backed fabric air bladders [5], and hydrogels [6]. In this work, we focus on pneumatic grippers constructed of fabric-strengthened air bladders (Fig. 1). When compared to rigid robotic grippers, two clear benefits emerge: 1) the gripper fingers can conform passively to differently-shaped objects, and 2) the gripper can be deflated, packed into a smaller volume, and then re-inflated with no loss in functionality. These benefits are advantageous in particular for volume- and weight-limited conditions, such as space exploration missions and assistive technologies.

Soft grippers are a relatively well-developed field [7]–[9] and many prototypes and even commercial products (Soft Robotics, Inc.; SuperReleaser) have been developed. Most of these grippers are controlled in an open-loop mode, where the gripper is commanded simply to either open or close, without feedback [9]. Similarly, the field of soft sensing is well-developed [10], [11], and commercial products (StretchSense, Inc.) have begun to emerge. The intersection of these two fields is less explored. It has been argued that soft grippers may operate using open-loop control because their intrinsic softness allows them to conform to different objects for a secure grasp, regardless of object shape, size, or mass [1]. However, this approach leads to a notable disadvantage: while an object may be securely grasped, the orientation of the object within the grasp is not known to the operator, limiting the utility of soft grippers in applications requiring precision grasping and manipulation of objects. Furthermore, challenges in accurately modeling the behavior of soft pneumatic actuators limit the performance of model-based open-loop control of such systems [9]. By adding sensors to a soft gripper, the configuration of the gripper fingers and the grasped object can be determined, enabling closed-loop control of the gripper.

Various researchers have begun to incorporate sensing alongside pneumatic actuation [2], [3], [12]–[20]. The sensors in these prototypes have been used to detect strain for state reconstruction and contact or pressure for environmental knowledge. Strain or bend sensors have been created using liquid metal resistive strain sensors [2], [3], [12]–[15], commercial piezoresistive flex

M. C.-S. Yuen and T. R. Lear are with the School of Mechanical Engineering, Purdue University, West Lafayette, IN 47907 USA (e-mail: yuenm@purdue.edu; lear.trevor@gmail.com).

H. Tonoyan and M. Telleria are with the Otherlab Pneubotics, San Francisco, CA 94110 USA (e-mail: henry@otherlab.com; mtelleri@mit.edu).

R. Kramer-Bottiglio is with the School of Mechanical Engineering, Purdue University, West Lafayette, IN 47907 USA, and also with the School of Engineering and Applied Science, Yale University, New Haven, CT 06520 USA (e-mail: rebecca.kramer@yale.edu).

sensors [16], magnetic Hall effect sensors [17], coiled wire for inductance-based sensing [19]–[21] and flexible optical sensors [22]–[24]. Touch-sensitive sensors have used capacitive sensors with conductive fabric electrodes [18], capacitive sensors with ionic hydrogel electrodes [25], and liquid metal resistive pressure sensors [15]. The large majority of the works cited here utilize silicone elastomer to create a bending pneumatic actuator, allowing sensors to be embedded or adhered in place easily. While this securely affixes the sensors to the actuator, failure of a single component results in system failure because components cannot be replaced without tearing the silicone elastomer comprising the system.

The works cited above are focused on incorporating sensing to enable closed-loop control of soft systems. However, few systems have demonstrated robust feedback control strategies for soft grippers and soft pneumatic actuators. External cameras have been utilized to track various points on a continuum actuator to perform proportional-integral-derivative (PID) control of the actuator configuration [26]. Pneumatic pressure sensors have been used to demonstrate proportional feedback control of finger curvature in a soft glove orthosis [27]. This work was extended through the addition of optical fiber curvature sensors on each finger of the glove to perform hierarchical PID control on the finger curvature magnitude [23]. Inductance sensing integrated onto bellows actuators has been used to perform proportional control on the bend angle of the actuator platform [20]. Embedded piezoelectric transducers have been used for closed-loop PID control of the force output from a pneumatic vibrotactile skin [28]. These approaches utilize a variety of sensing modalities to perform PID feedback control of soft actuator systems, suggesting that with sufficient sensing capabilities, relatively simple control strategies may be used to perform closed-loop control of soft systems.

In this work, we instrumented a fabric-based pneumatic gripper with highly deformable, capacitive strain and pressure (force) sensors to determine the position of and contact forces along each of the gripper's fingers, respectively. Taking a modular approach, the sensors were adhered to removable fabric sleeves that fit over each gripper finger to facilitate sensor replacement upon design changes or sensor failure. We characterized the system to determine the strain sensors' response to the gripper configuration and the pressure sensors' response to load. Using this information, we performed several demonstrations to showcase the capabilities of the instrumented gripper: 1) pack-and-deploy operation, 2) grasp reconstruction, and 3) closed-loop position control. Through the pack-and-deploy operation, wherein the gripper was fully deflated, packed down, and then re-deployed with no change in operational capabilities, we demonstrated the resilience of the instrumented gripper despite the large deformations incurred in this task. We then showed that we can reconstruct the position of and load on each of the gripper fingers during a grasping task. Finally, we used the strain sensor information to perform proportional closed-loop control of the gripper finger position. With the instrumented gripper system presented here, we progress towards more precise grasps and finer manipulation capabilities without sacrificing the benefits of soft grippers.
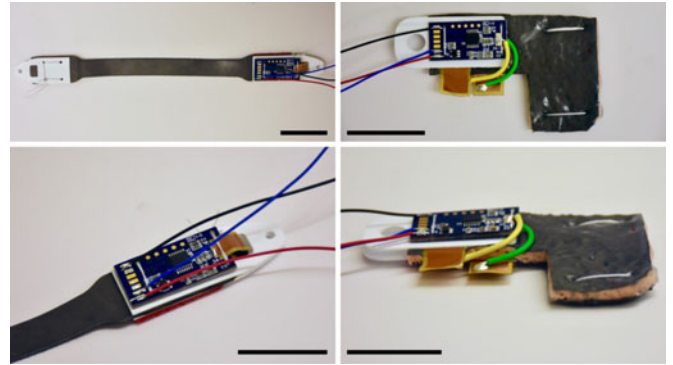

Fig. 2. Photos of the sensors. A strain sensor is shown in the left column and a pressure sensor is shown in the right column. The full sensors are shown in the top row and a close-up of the interface is shown in the bottom row. The signal conditioning electronics (blue circuit boards) are interfaced to the sensors via copper-clad polyimide strips. White polystyrene tabs hold the copper strips onto the surface of the sensors' electrodes and also serve as the mechanical interface region between the sensor body and the gripper. The scale bars indicate 3 cm.

II. EXPERIMENTAL SETUP

A. Sensors

We fabricated two types of sensors in this work: strain and pressure sensors (Fig. 2). The sensor technology presented here is closely based on our previous work [29]. The sensors were constructed as deformable parallel-plate capacitors that change in capacitance with applied strain or pressure. In [29], we demonstrated that the sensors have no change in performance over tens of thousands of cycles and can withstand up to 375% strain before failing due to degradation of the electrode material. These characteristics make the sensors well-suited for repeated use applications and allow for the sensors to be kept affixed to the gripper during pack-and-deploy situations.

Both the strain and pressure sensors were fabricated using primarily silicone elastomer (DragonSkin 10 Slow, Smooth-On). The two conductive layers were a composite material of 10wt% expanded intercalated graphite dispersed into silicone elastomer [29]; the dielectric layers were composed of non-conductive silicone elastomer. The strain sensors were fabricated by first rod-coating a film of the composite material, followed by native silicone to form the dielectric layer once the first layer had cured. The film was then folded in half, bonding the silicone dielectric layer to itself, to form the capacitive structure. Sensors were cut out of the larger film with a laser cutter (VLS 2.30, Universal Laser Systems).

For the pressure sensors, the electrode and dielectric layers were made separately. The electrode layer was made as before by rod-coating conductive composite material into a film. To fabricate the dielectric layer, silicone foam was made by mixing in sugar pellets (Colorcon Suglets) of four size regimes into uncured silicone elastomer. The quantities by mass were: 44 g silicone, 40 g 1400–1700 μm, 20 g 850–1000 μm, 30 g 500–600 μm, and 40 g 250–355 μm sugar pellets. The mixture was cast into a $\approx$5 mm thick sheet, followed by dissolving out the sugar pellets with hot water in a bath sonicator after curing. This process resulted in a very soft, porous silicone foam with a void volume fraction of 57.7% $\pm$ 2.6% (95% confidence). The
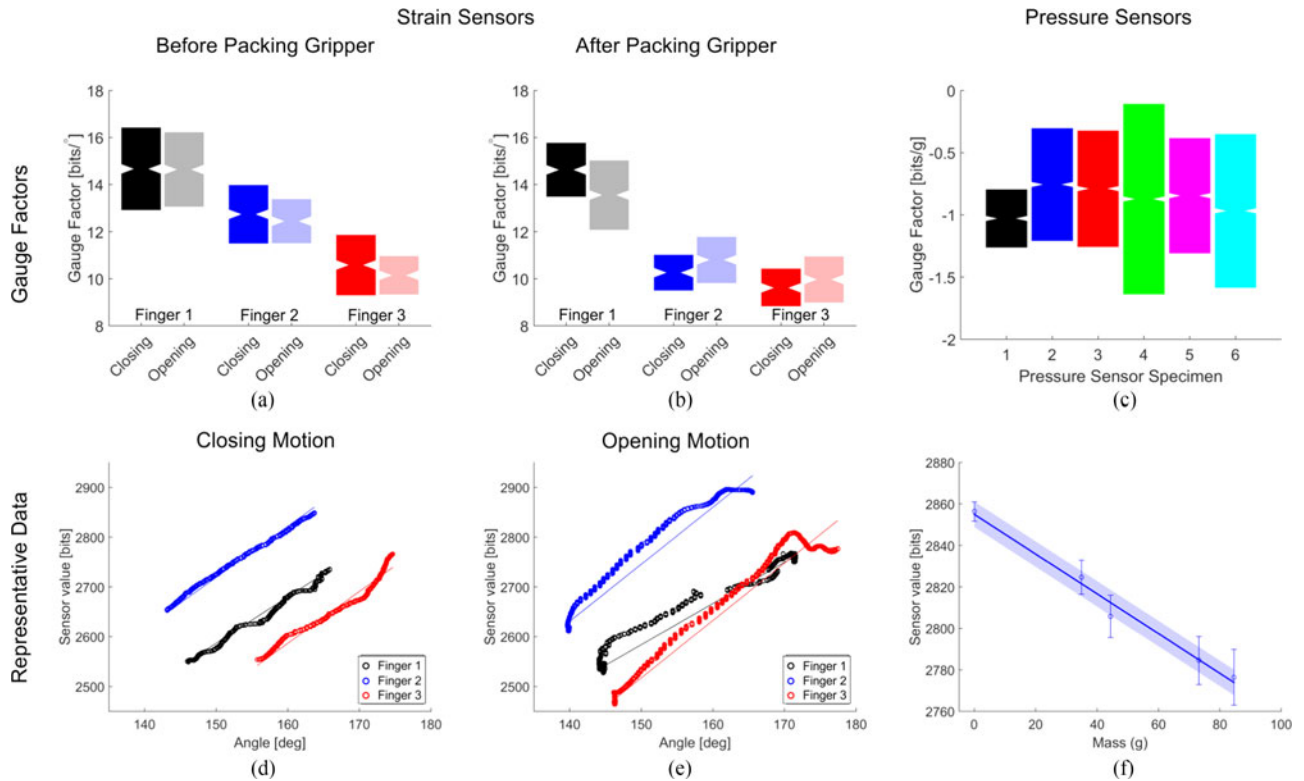
Fig. 3. Results of the calibration tests for the strain sensors and pressure sensors. (a) and (b) Strain sensor gauge factors (n = 3) during gripper opening and closing both before (a) and after (b) packing and re-deploying the sensors. (c) Pressure sensor gauge factors (n = 6). All gauge factors were calculated from a linear regression fit across the captured data. The notch indicates the mean gauge factor; the upper and lower bounds of the box indicate the 95% confidence about the mean. (d)–(f) Representative plots of calibration data and their regression lines: (d) plot of strain sensor outputs with respect to the ground truth joint angles while closing the gripper, (e) plot of strain sensor outputs with respect to the ground truth joint angles while opening the gripper, and (f) plot of a single pressure sensor's output with respect to the masses of various wooden blocks placed onto the sensor; the cloud around the fit line indicates 95% confidence bounds of the regression.

conductive film was then glued onto both sides of the dielectric layer using a 50 μm layer of uncured silicone elastomer.

After fabricating the sensor bodies, copper film was secured onto the electrodes by sewing polystyrene tabs on either side of the sensor. The copper film was then soldered onto signal conditioning boards [29] used to interrogate the sensors' capacitance. Finally, we affixed the sensors to off-the-shelf compression sleeves using adhesive-backed Velcro at the polystyrene tabs. This modular system enabled us to replace sensors quickly without compromising the entire system.

B. Gripper

The gripper consisted of three fingers attached to a rigid base. There were two sets of bladders in the gripper: one for closing the gripper by causing all the fingers to curl inwards, and one to open the gripper by forcing all the fingers to extend straight. The bladders were made by encasing airtight vinyl pouches inside of ripstop nylon for strength. They were sewn to the inner surface of the fabric comprising each finger: the closing bladder was sewn to the back of the fingers, and the opening bladder was sewn to the inside of the finger. The closing and opening bladders were connected via tubing such that for the entire gripper, there was a single inlet for closing and a single inlet for opening the gripper. At any one time, only a single bladder is inflated.

The gripper valves were plumbed such that when transitioning from one state to another, one bladder fills as the other vents.

III. IN SITU SENSOR CHARACTERIZATION

We characterized the strain and pressure sensors after installing them on the gripper (Fig. 3). We compared the strain sensor output to truth data generated by a motion capture system and the pressure sensor output to truth data generated by placing known weights on the sensors. Both types of sensors had a linear relationship with respect to their inputs and thus, we report their gauge factors (Fig. 3(a)–(c)). These linear regression results were then used to perform gripper proprioception and grasped object localization in the applications discussed further in this letter.

A. Strain Sensors

For the strain sensors, we found the relationship between the sensor output and joint angle of each finger (approximated as a 1DoF hinge joint) (Fig. 3(a), (b), (d), (e)). Truth data (finger joint angles) were generated using a motion capture system where three motion capture markers were placed on each finger: near the base, in the middle, and at the finger tip. We compared the results across two conditions, for a total of four categories: 1) during opening and closing phases, and 2)

before and after deflation and packing of the gripper (pack-and-deploy). Fig. 3(a) reports gauge factors from data captured prior to packing; Fig. 3(b) reports gauge factors from data captured after deflating, compacting the gripper down, and re-deploying. The representative datasets plotted in Fig. 3(d) (closing) and Fig. 3(e) (opening), show that the sensor response to joint angle can be reasonably approximated as a linear relationship (all linear regression R^2 values were between 0.963 and 0.998). We first compared the gauge factors of each sensor during the opening and closing phases in Fig. 3(a) and (b) and found that there was little difference between the gauge factors during the closing and opening phases for each sensor, particularly prior to packing. We hypothesize that the differences in gauge factor between the opening and closing phases are due to reduced contact between the sensor and the finger during the opening phase relative to the closing phase. The difference in sensor behavior can also observed in the plots in Fig. 3(d) and (e). Because the sensors are capacitors, changes in the near electric field, including contact with other bodies, will affect the sensor reading. Shielding the sensors would aid in mitigating the effect of near electric field on the sensor signal.

We also compared the gauge factors of the strain sensors found before (Fig. 3(a)) and after (Fig. 3(b)) a pack-and-deploy sequence. One benefit of inflatable fabric grippers that distinguishes them from rigid grippers is their ability to be packed into a much smaller volume and then deployed without change in function. In order for the sensors to be compatible with the packing and deployment of the gripper, they needed to withstand large amounts of deformation outside their normal operating range. The metric for this test was change in gauge factor before and after packing. While two of the sensors clearly remained stable throughout the packing event, the sensor on finger 2 appeared to display different behavior. We do not believe that this is due to damage to the sensor itself because the confidence bounds on the gauge factor are of comparable width before and after the packing. Rather, we hypothesize that this change is due to shifted and altered mechanical and electrical interfaces. Work towards directly integrating the sensors into the fabric comprising the gripper is a potential solution to this interfacing problem. The fabric would hold the sensor with more stability over large deformations, and would serve as an anchor point to which electrical interfaces may be secured more robustly.

B. Pressure Sensors

The pressure sensors were calibrated by placing wooden blocks of known weights onto them, yielding a highly linear relationship between the pressure sensor response and applied load. The gauge factors of all pressure sensors are reported in Fig. 3(c) and a representative dataset is shown in Fig. 3(f). The sensors were all tested *in situ* in their respective positions on the inflated gripper to account for the stiffness of the gripper finger in the pressure sensor output. Sensors 1, 4, 6 were located in the middle of the finger; sensors 2, 3, 5 were located at the finger tip. We hypothesize that the differences in the gauge factors, reported in Fig. 3(c), are due to minor differences in the stiffness of the dielectric layers in different sensors. Further, we hypothesize that the variation in width of the confidence
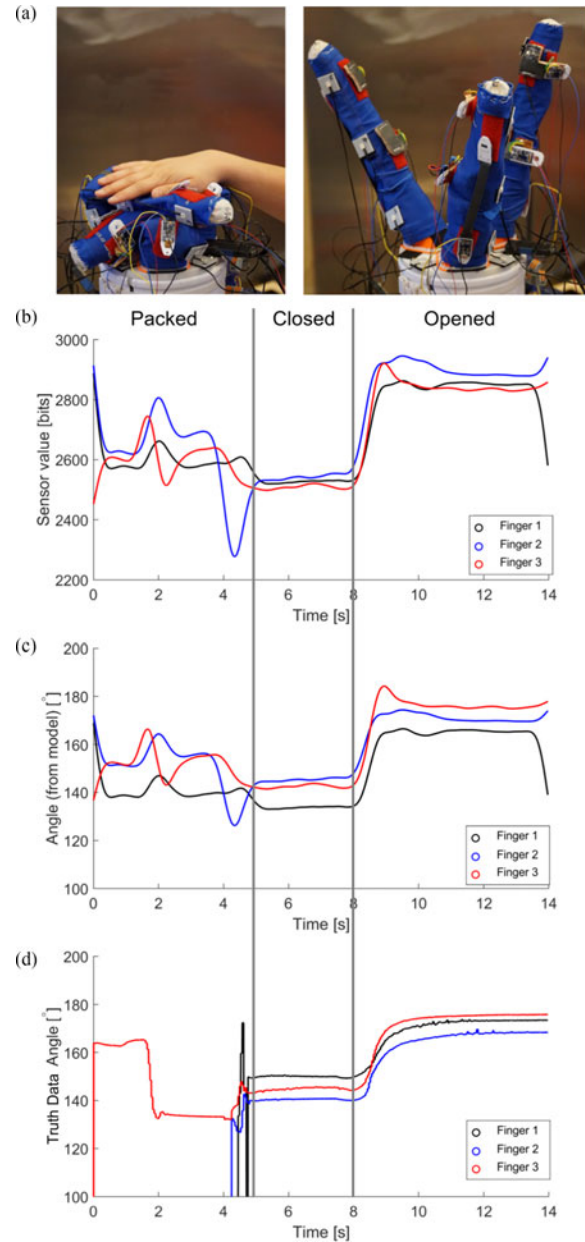

Fig. 4. State reconstruction during a pack-and-deploy sequence. (a) Photos of the gripper in the packed (left) and open state (right). (b)–(d) Plots corresponding to the gripper first in a packed condition (0–5 s), followed by deployment into a closed position (5–8 s), and then actuating to an open position (8–14 s). (b) Sensor output filtered with a noncausal zero-phase digital filter. (c) Joint angle of each gripper finger determined using the calibration equations found previously (Section 3). (d) Ground truth joint angle of each gripper finger as found using a motion capture system. The plots in (c) and (d) can be compared to assess the performance of the sensory sleeves against ground truth.

bounds is due to experimental variation in placing the blocks in the same location on the sensors, changing the effective area that was compressed by the load, thus changing the measured capacitance.

IV. APPLICATIONS

A. State Reconstruction During Pack-and-Deploy Sequence

Fig. 4 demonstrates a full pack-and-deploy sequence. Representative states during the pack-and-deploy sequence are shown

in Fig. 4(a). In the plots shown in Fig. 4(b)–(d), t = 0–5 s, t = 5–8 s, and t = 8–14 s correspond to a packed state, a closed gripper state, and a fully open gripper state, respectively. Fig. 4(b) shows the raw sensor outputs during the sequence, Fig. 4(c) shows the expected finger position calculated from the raw sensor data and post-packing calibration curves, and Fig. 4(d) shows truth data for the entire sequence generated via motion capture.

In comparing Fig. 4(c) and (d), the reconstructed finger position matches well to the joint angles from the motion capture system after the gripper is re-deployed. During the transition from a packed state to a deployed state, the sensor readings are not correlated with the actual finger position. However, this is not a problem as the goal of this test was to ensure that we can still use the sensor readings when the gripper is re-deployed after having been deflated and packed down. More importantly, after the packed phase, we found that the reconstructed joint angle tracks well to the ground truth joint angle (Fig. 4(c) and (d), respectively), reinforcing the result that the gripper and strain sensors are resilient to the larger strains that occur while the gripper is in a deflated and packed configuration.

B. State Reconstruction During Grasping Tasks

Using the calibration results, we tested the sensors in a grasping scenario. We directed the gripper to grasp various objects to simultaneously verify that the pressure sensors could detect an object, and that the strain sensors could be used to estimate the state of the gripper fingers. As in previous tests, the pressure sensors were placed on the inside of the fingers at the tip and at the center of each finger, and the strain sensors were affixed along the outside of the fingers.

Fig. 5 shows state reconstruction of the gripper fingers during a grasping task. In this example, the gripper grasped and then released a water bottle. Fig. 5(a) shows the raw pressure sensor data and Fig. 5(b) shows the expected normal load (presented as mass) of the grasped object calculated from the raw sensor data and calibration curve. The pressure sensors clearly detect the water bottle being evenly gripped at the tips of the gripper fingers. The sensors at the tips of the fingers (black, red, and blue traces) show an increase in load corresponding to the gripping of the water bottle. Upon releasing the water bottle, these same sensors show a decrease in load that corresponds to the water bottle sticking to the sensors as the gripper opens, resulting in the electrode layers being pulled further apart and the capacitance to decrease momentarily before the object is fully released. Fig. 5(c) shows images of the gripper in an open state and closed state around the object.

Fig. 5(d) shows the raw strain sensor data, Fig. 5(e) shows the expected gripper finger bend angles calculated from the raw data using the post-packing calibration curves, and Fig. 5(f) shows the actual figure bend angles as found from motion capture (truth data). While the reconstructed joint angle values do not match perfectly to the truth data, the strain sensors do track the relative motion of the fingers across the opened and closed states, therefore yielding useful information about the general state of the fingers and overall gripper. We believe that discrepancies between the measured state and true state are due to the fingers

bending very close to the base, which is recorded by the motion capture system, but is outside the ideal range of the sensor measurement in the current configuration.

C. Closed-Loop Control

Using the strain sensors mounted on the fingers, we demonstrated closed-loop control of the fingers. The control system consisted of nested proportional controllers (Fig. 6). The outer position control loop generated the desired air pressures in the finger bladders based on the difference between the commanded and measured finger position, determined via the strain sensor value. The positional set-point was based on a single sensor value because all three fingers were plumbed together. We used two different gains to calculate the air pressure commands depending on whether the gripper was closing or opening because much less pressure was need for closing compared to opening the gripper due to biases in the actual construction of the finger. The pressure commands were then fed into the inner loops to independently control the air pressure in the opening and closing bladders.

The plots in Fig. 7 show two representative runs: column (a) shows the gripper cycling through a closed and opened state, and column (b) shows the gripper gradually stepping from a closed state to an opened state. In Fig. 7, the top row shows the setpoint (blue), and the sensor output from a single finger (red), and the bottom row shows the corresponding air pressure inside the bladders of the gripper. It is important to note that the gripper was originally designed to have two states: open and closed. Therefore the pressure-to-position relationship is poor, which makes it difficult to control the position of the fingers using only air pressure data from the two chambers. By introducing strain sensors into the control loop, we overcame this limitation in achieving positional control of the gripper.

For this portion of the work, we changed the approach we took to measure capacitance. The signal conditioning boards previously used exhibited a very low frequency oscillation at around 2.5 Hz which made them challenging to use for real-time closed-loop control. In non real-time tests the oscillation was removed by using a noncausal zero-phase digital filter. In real-time control however, low-pass filtering the signal at such a low frequency resulted in unacceptable phase lag and delay. For real-time control, capacitance measurement was re-implemented directly on the gripper's control board. The capacitive sensors were charged using larger currents which resulted in less susceptibility to noise caused by small external electrical fields. In addition, measurements could be made directly on the gripper's control board, instead of being transmitted over an analog channel as they previously were, thus eliminating the need for an additional analog-to-digital conversion.

After improving the electronics, we used the capacitive strain sensors for position feedback and pneumatic valves to control actuation. As before, the system was plumbed so that all three fingers were controlled as one. Enfield LS-V25s 5 port proportional valves were used to control the pressure in the gripper bladders. One valve controlled pressure to the bladder that opens the finger and the other valve was connected to the bladder that
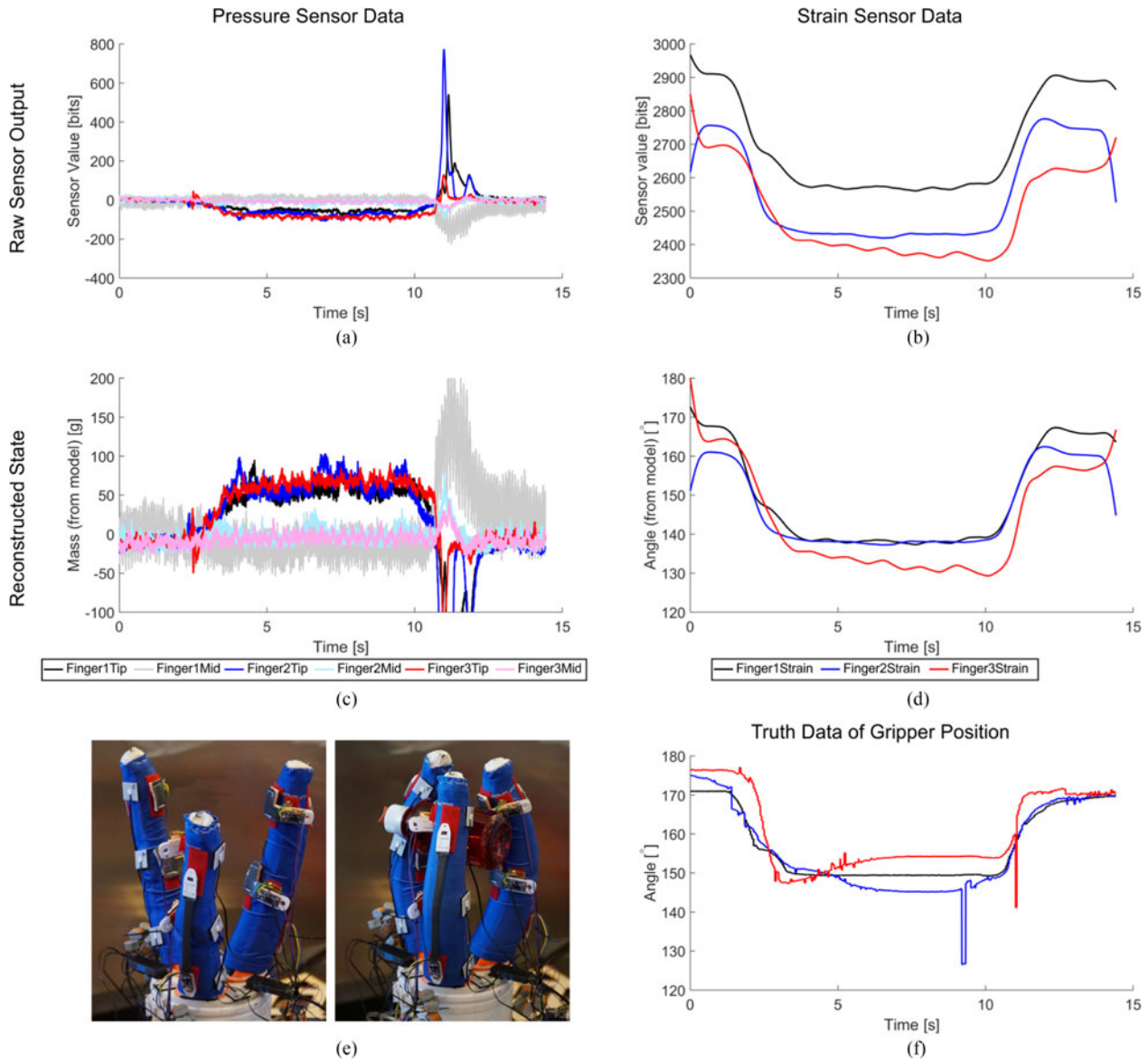
Fig. 5. State and contact estimation during an object grasping sequence. (a) Raw pressure sensor responses. (b) Reconstructed mass experienced by each pressure sensor, as calculated from the calibration curves. (c) Photos of the gripper in its open state and closed state around a water bottle. (d) Raw strain sensor responses. (e) Reconstructed joint angle of each finger, as calculated from the calibration curves. (f) Angles of each finger as determined by the motion capture system. The spikes in the trace arise from loss of line of sight to one or more markers.
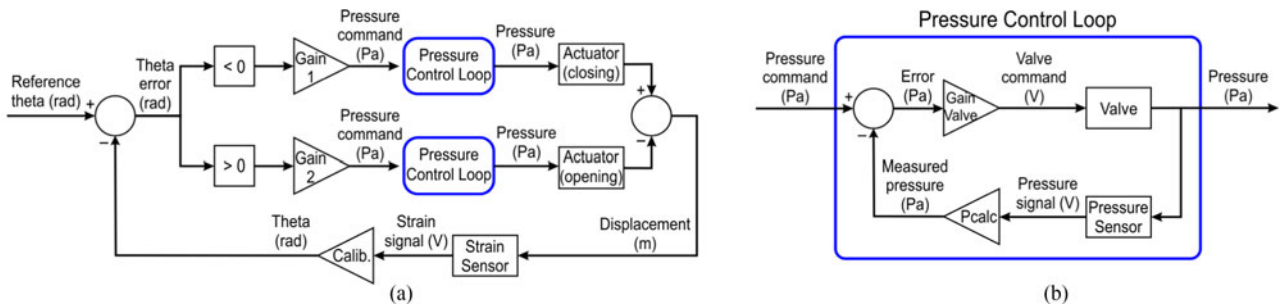

Fig. 6. Block diagram of the control scheme. As shown in (a), the controller consists of nested proportional controllers. The outer loop controls the finger positions, and the inner loops (b) control the pressure supplied to the gripper's two bladders. Gain1, Gain2, and GainValve are proportional gain constants. In a), Calib. refers to the linear regression equation relating finger angle to sensor strain value found in the calibration of the sensors. In b), Pcalc. refers to the manufacturer-specified conversion from voltage to pressure value.
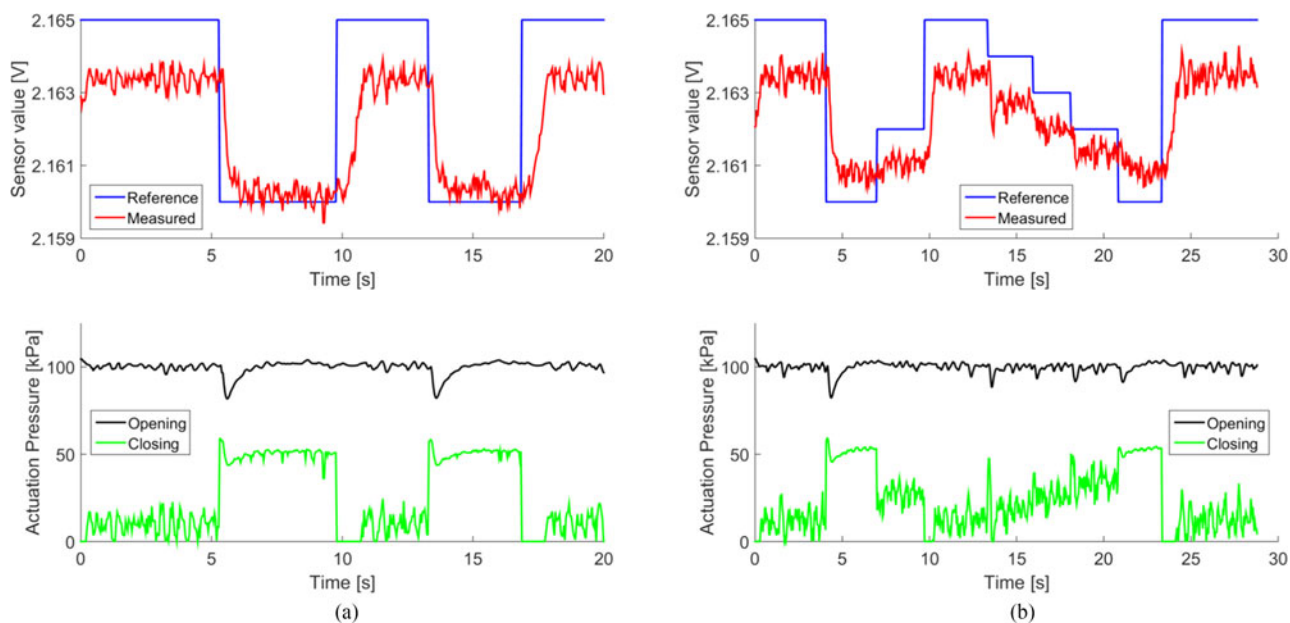
Fig. 7.   Closed-loop control of the gripper. Column (a) shows the gripper performing two cycles of closing and opening, then finally closing. Column (b) shows the gripper stepping from a closed state gradually to an open state. The top plots show the reference setpoint for the strain sensors in blue, and the measured strain sensor values in red. The error generated between these two values are used to trigger the pneumatic valves to fill or vent as needed. The bottom plots show the pressure inside the opening and closing bladders.

closes the finger. The pressure of the inner and outer bladders were measured using Honeywell 0-15psi range pressure sensors.

We note that the system does not fully match the setpoint values, however the gripper is clearly responding to changes in the setpoint. We believe that further work in four areas will improve the performance of the system: (i) using a more sophisticated control strategy, for example, using a PI or PID controller rather than just a proportional controller [20], (ii) implementing the sensors on a joint which is designed to have a better pressure-to-position relationship, (iii) further improving the signal-to-noise ratio of the sensors through the signal conditioning electronics, (iv) improved interfacing of the sensors with the host system.

V. CONCLUSION AND FUTURE WORK

In conclusion, we have demonstrated progress towards closed-loop control of soft robotic grippers using highly deformable capacitive sensors on a fabric-based pneumatic gripper for state measurement and object detection. The sensors were constructed as parallel plate capacitors with expanded graphite and silicone composite serving as the electrode material and native silicone or silicone foam serving as the dielectric material. By using a silicone-based construction, the sensors were resilient to large strains encountered during pack-and-deploy operations wherein the gripper was fully deflated and then redeployed. The strain sensors maintained a linear response under closing and opening operations and the pressure sensors had a linear response to applied normal load, both before and after deflation and re-deploying. Using these sensors, we demonstrated three unique applications of fabric-based pneumatic grippers: pack-and-deploy operations, grasping of oddly-shaped objects, and closed-loop position control of the gripper.

Future work on this system includes improvement of the signal conditioning electronics and sensor design, for an increased signal-to-noise ratio. Further shielding on the sensors by wrapping a grounding layer around the entire sensor body will reduce the effect of near electric field on the sensor signal. As mentioned previously, increasing the charge-discharge current used to interrogate the sensors will also improve the signal-to-noise ratio, as well as enable higher measurement frequency. Another improvement would be to increase the spatial density of both the strain and pressure sensors, so as to measure compound curvatures and more points of contact, respectively. Most crucially, an additional strain sensor spanning the junction between the finger and the base will improve the accuracy of the state reconstruction of the gripper. Increasing the density and areal coverage of pressure sensors along the inside of the fingers will yield a better understanding of what the gripper has grasped. Finally, underlying the need for more sensors is the need for better physical interfaces. In order to accommodate more sensors, the sensors may be directly fabricated into the fabric itself. Not only will this allow the sensing density to increase, the repeatability of the sensor output should increase as the sensors will not change position during operation.

We will also explore more sophisticated control strategies to improve on the performance of the closed-loop control shown here. Our first step here is to implement integral and derivative terms for PID control, as demonstrated by other researchers. Another possibility is to control the pressure differential between the opening and closing bladders, such that they serve as antagonistic actuator pairs, similar to the bicep-tricep muscle pair on the human body.

With this work, we have advanced the capabilities of soft robotic grippers. Previous gripper devices have relied upon

passive conforming to securely grasp objects. By instrumenting soft grippers with soft strain sensors and pressure sensors, we can achieve closed-loop control during a grasping task to grip with known position, object orientation, and contact force, thus furthering the capabilities of soft robotic grippers.

REFERENCES

[1] F. Ilievski, A. D. Mazzeo, R. F. Shepherd, X. Chen, and G. M. Whitesides, "Soft robotics for chemists," *Angew. Chemie*, vol. 123, no. 8, pp. 1930–1935, Feb. 2011.

[2] R. A. Bilodeau, E. L. White, and R. K. Kramer, "Monolithic fabrication of sensors and actuators in a soft robotic gripper," in *Proc. 2015 IEEE/RSJ Int. Conf. Intell. Robots Syst.*, 2015, pp. 2324–2329.

[3] N. Farrow and N. Correll, "A soft pneumatic actuator that can sense grasp and touch," in *Proc. 2015 IEEE/RSJ Int. Conf. Intell. Robots Syst.*, 2015, pp. 2317–2323.

[4] J. H. Low *et al.* "Hybrid tele-manipulation system using a sensorized 3-D-printed soft robotic gripper and a soft fabric-based haptic glove," *IEEE Robot. Autom. Lett.*, vol. 2, no. 2, pp. 880–887, Apr. 2017.

[5] R. Niiyama, D. Rus, and S. Kim, "Pouch motors: Printable/inflatable soft actuators for robotics," in *Proc. 2014 IEEE Int. Conf. Robot. Autom.*, May 2014, pp. 6332–6337.

[6] H. Yuk, S. Lin, C. Ma, M. Takaffoli, N. X. Fang, and X. Zhao, "Hydraulic hydrogel actuators and robots optically and sonically camouflaged in water," *Nature Commun.*, vol. 8, Feb. 2017, Art. no. 14230.

[7] S. Kim, C. Laschi, and B. Trimmer, "Soft robotics: A bioinspired evolution in robotics," *Trends Biotechnol.*, vol. 31, no. 5, pp. 287–294, May 2013.

[8] D. Rus and M. T. Tolley, "Design, fabrication and control of soft robots," *Nature*, vol. 521, no. 7553, pp. 467–475, 2015.

[9] P. Polygerinos *et al.*, "Soft Robotics: Review of fluid-driven intrinsically soft devices; manufacturing, sensing, control, and applications in human-robot interaction," *Adv. Eng. Mater.*, 2017.

[10] S. Bauer, S. Bauer-Gogonea, I. Graz, M. Kaltenbrunner, C. Keplinger, and R. Schwdiauer, "25th anniversary article: A soft future: From robots and sensor skin to energy harvesters," *Adv. Mater.*, vol. 26, no. 1, pp. 149–162, Jan. 2014.

[11] J. Case, M. Yuen, M. Mohammed, and R. Kramer, "Sensor skins: An overview," in *Stretchable Bioelectronics for Medical Devices and Systems* (Ser. Microsystems and Nanosystems), J. A. Rogers, R. Ghaffari, and D.-H. Kim, Eds. Berlin, Germany: Springer, 2016, pp. 173–191.

[12] N. Farrow, Y. Li, and N. Correll, "Morphological and embedded computation in a self-contained soft robotic hand," arXiv:1605.00354, May 2016.

[13] Y. L. Park, B. r. Chen, C. Majidi, R. J. Wood, R. Nagpal, and E. Goldfield, "Active modular elastomer sleeve for soft wearable assistance robots," in *Proc. 2012 IEEE/RSJ Int. Conf. Intell. Robots Syst.*, Oct. 2012, pp. 1595–1602.

[14] Y.-L. Park and R. J. Wood, "Smart pneumatic artificial muscle actuator with embedded microfluidic sensing," in *Proc. SENSORS*, 2013, pp. 1–4.

[15] J. Morrow *et al.*, "Improving soft pneumatic actuator fingers through integration of soft sensors, position and force control, and rigid fingernails," in *Proc. 2016 IEEE Int. Conf. Robot. Autom.*, May 2016, pp. 5024–5031.

[16] B. S. Homberg, R. K. Katzschmann, M. R. Dogar, and D. Rus, "Haptic identification of objects using a modular soft robotic gripper," in *Proc. 2015 IEEE/RSJ Int. Conf. Intell. Robots Syst.*, Sep. 2015, pp. 1698–1705.

[17] M. Luo *et al.*, "Toward modular soft robotics: Proprioceptive curvature sensing and sliding-mode control of soft bidirectional bending modules," *Soft Robot.*, vol. 4, no. 2, pp. 117–125, Jun. 2017.

[18] N. Farrow, L. McIntire, and N. Correll, "Functionalized textiles for interactive soft robotics," in *Proc. 2017 IEEE Int. Conf. Robot. Autom.*, May 2017, pp. 5525–5531.

[19] W. Felt, K. Y. Chin, and C. D. Remy, "Contraction sensing with smart Braid McKibben muscles," *IEEE/ASME Trans. Mechatronics*, vol. 21, no. 3, pp. 1201–1209, Jun. 2016.

[20] W. Felt *et al.*, "An inductance-based sensing system for bellows-driven continuum joints in soft robots," in *Proc. Robot., Sci. Syst.*, Cambridge, MA, USA, Jul. 2017, doi: 10.15607/RSS.2017.XIII.027.

[21] W. Felt, M. Suen, and C. D. Remy, "Sensing the motion of bellows through changes in mutual inductance," in *Proc. 2016 IEEE/RSJ Int. Conf. Intell. Robots Syst.*, Oct. 2016, pp. 5252–5257.

[22] H. Zhao, K. O'Brien, S. Li, and R. F. Shepherd, "Optoelectronically innervated soft prosthetic hand via stretchable optical waveguides," *Sci. Robot.*, vol. 1, no. 1, Dec. 2016, Art. no. eaai7529.

[23] H. Zhao, R. Huang, and R. F. Shepherd, "Curvature control of soft orthotics via low cost solid-state optics," in *Proc. 2016 IEEE Int. Conf. Robot. Autom.*, May 2016, pp. 4008–4013.

[24] S. Sareh, Y. Noh, M. Li, T. Ranzani, H. Liu, and K. Althoefer, "Macrobend optical sensing for pose measurement in soft robot arms," *Smart Mater. Struct.*, vol. 24, no. 12, 2015, Art. no. 125024.

[25] S. S. Robinson *et al.*, "Integrated soft sensors and elastomeric actuators for tactile machines with kinesthetic sense," *Extreme Mech. Lett.*, vol. 5, pp. 47–53, Dec. 2015.

[26] A. D. Marchese, K. Komorowski, C. D. Onal, and D. Rus, "Design and control of a soft and continuously deformable 2D robotic manipulation system," in *Proc. 2014 IEEE Int. Conf. Robot. Autom.*, May 2014, pp. 2189–2196.

[27] P. Polygerinos, Z. Wang, K. C. Galloway, R. J. Wood, and C. J. Walsh, "Soft robotic glove for combined assistance and at-home rehabilitation," *Robot. Auton. Syst.*, vol. 73, pp. 135–143, Nov. 2015.

[28] H. A. Sonar and J. Paik, "Soft pneumatic actuator skin with piezoelectric sensors for vibrotactile feedback," *Front. Robot. AI*, vol. 2, p. 38, 2016, doi: 10.3389/frobt.2015.00038.

[29] E. L. White, M. C. Yuen, J. C. Case, and R. K. Kramer, "Low-cost, facile, and scalable manufacturing of capacitive sensors for soft systems," *Adv. Mater. Technol.*, vol. 2, 2017, Art. no. 1700072.